

# Intracavity laser spectroscopy of laser-spark excited molecules

T.M. Petrova, L.N. Sinita, and A.M. Solodov

*Institute of Atmospheric Optics,  
Siberian Branch of the Russian Academy of Sciences, Tomsk*

Received November 18, 2005

The absorption spectra of iron, chrome, manganese, zirconium, and industrial graphite, excited by a laser spark, were investigated with the use of intracavity laser spectrometer operating in the 1.06 micron region. C<sub>2</sub> absorption spectra were identified and rotational lines of the transitions 3–0, 4–1, and 5–2  $b^3\Sigma_g^- - a^3\Pi_u$ , as well as 2–1, 1–0  $A^1\Pi_u - X^1\Sigma_g^+$  were determined.

The latter part of the XX century is characterized by intensive development of laser-induced breakdown spectroscopy (LIBS), i.e. the method of investigation of laser-spark excited matters. The basis for the technique is the fact that the laser radiation impact on a solid target causes the target matter volatilization and the plasma initiation, which radiation can be recorded by spectral instruments. The 694 nm ruby laser generating 50-ns pulses was used in the first experiments.<sup>1</sup> The technique did not receive a wide acceptance at that time because of difficulties in controlling and obtaining stable generation parameters from pulse to pulse.

The advent of excimer and Nd:YAG-lasers, as well as sensitive radiation detectors favored a rapid development of the LIBS technique, which has found a wide diversity of applications in different areas: the real-time data analysis, combustion diagnostics, biology, detection of trace gas concentrations, control for environmental pollution, etc.<sup>2–5</sup> A great deal of papers was devoted to the LIBS techniques, but they mostly dealt with the low resolution radiation spectra. The intracavity (IC) spectroscopic technique opens new prospects in this area. Due to high absorption sensitivity and high spectral resolution, the IC-spectroscopy allows the study of weak absorption spectra of laser-spark excited molecules. However, very few works are known today, which combine the both methods. In these works, plasma parameters are studied with the use of the visible IC spectrometers.<sup>6,7</sup>

In this work we describe a 1.06  $\mu\text{m}$  spectrometer based on the IC technique, which is intended for recording absorption spectra of laser-spark excited molecules. The spectrometer operation is exemplified by recording absorption spectra of metal oxides and industrial graphite. We have recorded many new lines in the absorption spectra and identified the C<sub>2</sub> molecule absorption spectrum.

## Technique

The IC spectroscopy technique is based on the damping of the lasing spectrum in individual frequency

ranges corresponding to absorption lines of a matter inside the cavity.<sup>8</sup> The lasing spectrum has sharp dips at the absorption line frequencies, which can be recorded by some ordinary spectral instruments. The equation describing radiation attenuation due to absorption of the matter inside the laser cavity has the form

$$J(\nu, t) = J(\nu, t_0) \exp[-K(\nu)L_{\text{ef}}], \quad (1)$$

$$L_{\text{ef}} = ctL_a / L_c,$$

where  $J(\nu, t_0)$  is the laser spectrum formed to the beginning of the lasing pulse;  $K(\nu)$  is the spectral absorbance;  $c$  is the light velocity;  $t$  is the quasi-continuous lasing duration;  $t_0$  is the lasing duration at the initial moment;  $L_a$  is the absorbing layer length;  $L_c$  is the cavity length.

The laser simulates a multipass absorption cell with much longer effective length  $L_{\text{ef}}$ , where attenuation of the laser radiation intensity due to losses is compensated by its intensification during the radiation pass through the laser active medium. At a quasi-continuous lasing duration of 1 ms and total filling of the cavity with the absorbing matter,  $L_{\text{ef}}$  can attain 300 km.

According to data from Ref. 9 and our observations, laser-induced sparks can attain 1 cm in diameter depending on the target type and the laser power. Following Eq. (1),  $L_{\text{ef}}$  in this case is equal to 3 km; this allows recording very weak spectral lines with absorption coefficients of  $10^{-7} \text{ cm}^{-1}$ .

## Experimental setup

The block diagram of the experimental setup is shown in Fig. 1. The spectrometer consists of a channel for recording absorption spectra by the IC technique and a channel for exciting molecules in the laser spark.

A multimode flash-lamp pumped Nd-glass laser and high-resolution spectral device with an optical multichannel analyzer were used in the spectrum recording channel. The free-running laser had a smooth

broadband spectrum in the range 9360–9450  $\text{cm}^{-1}$ . Lasing pulse duration was 1000  $\mu\text{s}$ . A DFS-8 diffraction spectrograph with a 2650 mm focal length and 12th-order diffraction grating of 150 lines/mm was used in recording the laser spectrum. The IC technique allows weak absorption lines to be studied with a resolution of 0.03  $\text{cm}^{-1}$ . This part of the spectrometer has been described in Refs. 10 and 11 in more detail.

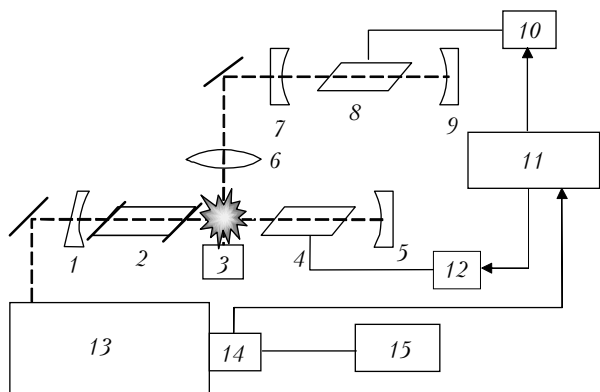


**Fig. 1.** Block diagram of the experimental setup: mirrors of the IC spectrometer cavity (1 and 6), optical cell with water vapor (2), target (3), active element (4), spherical lens (5), mirrors of the exciting laser cavity (7 and 9), active element (8), triggers for the main and exciting lasers (10 and 12), oscillograph (11), DFS-8 diffraction spectrograph (13), CCD photodetector (14), and PC (15).

A similar Nd laser with a pulse duration of 1000  $\mu\text{s}$  in basis and a power of 1 J was used in the molecule-excitation channel. Radiation of the Nd laser, focused on the target (the lens focal length of 150 mm), generated a spark on the recording laser cavity axis. The synchronization scheme allowed varying time delay between lasing pulses of the recording and main lasers from 0 to 2000  $\mu\text{s}$ . The target was irradiated at a room temperature. Different parts of the spark were studied by the target displacement normally to the resonator optical axis.

## Measurement results

Different oxides of elements from the 4th row of the periodic table (iron, chromium, manganese, and zirconium) and industrial graphite were the objects of the study.

1. *Metallic oxides.* When exciting oxides by laser sparks, strong absorption lines are observed in the laser spectrum. In this case, similar absorption spectra are observed for different oxides of the same chemical element (Fig. 2).

Similar results were obtained by the authors of Ref. 12 with the dye-laser IC spectrometer. They investigated products of gas-phase reactions proceeding under controllable discharge conditions. They have studied kinetics of formation of transition-metal monoxides and mononitrides, as well as have found and recorded new bands in electronic rovibrational spectra.

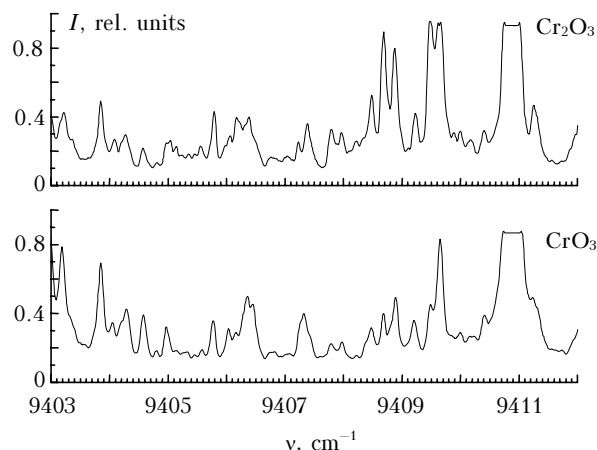


**Fig. 2.** IC spectrum of chromous oxides excited by laser spark in the 9403–9412  $\text{cm}^{-1}$  range.

We have recorded spectra of metal oxides in the 1  $\mu\text{m}$  range for the first time. At present, it is impossible to identify the recorded spectra, because exact values of vibrational constants for ground and excited states of these molecules are not available in literature.

2. *Graphite target.* There are many works on emission and absorption spectra of the  $\text{C}_2$  molecule,<sup>13,14</sup> which is a main component of hydrogen flame and other soot-forming systems. The  $\text{C}_2$  molecule is meant to be a transient element in the processes proceeding when producing diamond and diamond-like films. The  $\text{C}_2$  spectra were observed in radiation of carbon stars, comets, and interstellar clouds.

The  $\text{C}_2$  molecule is one of few diatomic molecules having two low electronic states, i.e. electronic ground state  $X^1\Sigma_g^+$  and the first triplet state  $a^3\Pi_u$  (Fig. 3).

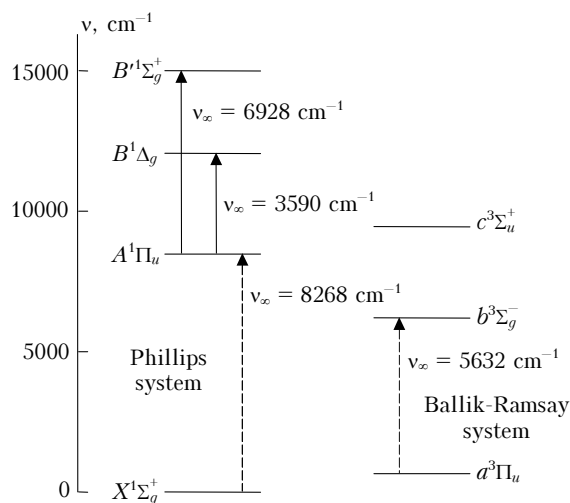


**Fig. 3.** Diagram of low-lying electronic states of the  $\text{C}_2$  molecule.

These states are spaced by a mere 630  $\text{cm}^{-1}$ ; their populations are quantitatively comparable. Two extra low-lying electronic states are known:  $b^3\Sigma_g^-$  centered at  $\sim 6434 \text{ cm}^{-1}$  and  $A^1\Pi_u$  centered at  $8391 \text{ cm}^{-1}$ .

Besides these low-lying electronic states, more than 14 electronic states of the  $C_2$  radical are observed,<sup>14</sup> which manifests themselves most frequently in emission spectra. There exist many systems of vibronic bands, the most known of which are the Swan band system ( $d^3\Pi_g - a^1\Pi_u$ ) with the band centered at  $19400\text{ cm}^{-1}$ ; Phillips system ( $A^1\Pi_u - X^1\Sigma_g^+$ ), centered at  $8268\text{ cm}^{-1}$ ; and Mulliken one ( $D^1\Sigma_u^+ - X^1\Sigma_g^+$ ) centered at  $43227\text{ cm}^{-1}$ .

The  $1\text{ }\mu\text{m}$  spectral range turned out to be studied insufficiently;<sup>15–18</sup> many lines, relating to the Ballik–Ramsay band system, were not recorded and identified due to their weak intensity. According to estimates, the lines belonging to different rotational branches of several vibronic transitions can fall into this range simultaneously. These transitions are  $A^1\Pi_u - X^1\Sigma_g^+$  (Phillips band system) and  $B^1\Sigma_g^+ - A^1\Pi_u$ , electronic states of which are singlet, as well as the  $b^3\Sigma_g^- - a^3\Pi_u$  transition (Ballik–Ramsay band system). To calculate the  $C_2$  spectrum, standard equations for energy levels of diatomic molecules and spectroscopic constants, obtained in Refs. 15–18, were used.

Figure 4 shows the IC spectrum of the laser with the graphite-target spark. Virtually total absorption is observed ( $\tau = 0\text{ }\mu\text{s}$  in Fig. 4) in the absence of a delay between pulses of the main and exciting lasers. The absorption begins to decrease with increasing delay and it is pronounced most clearly at a delay of about  $600\text{ }\mu\text{s}$ . At further increase of the delay ( $\tau > 800\text{ }\mu\text{s}$ ), only atmospheric air absorption lines are observed.

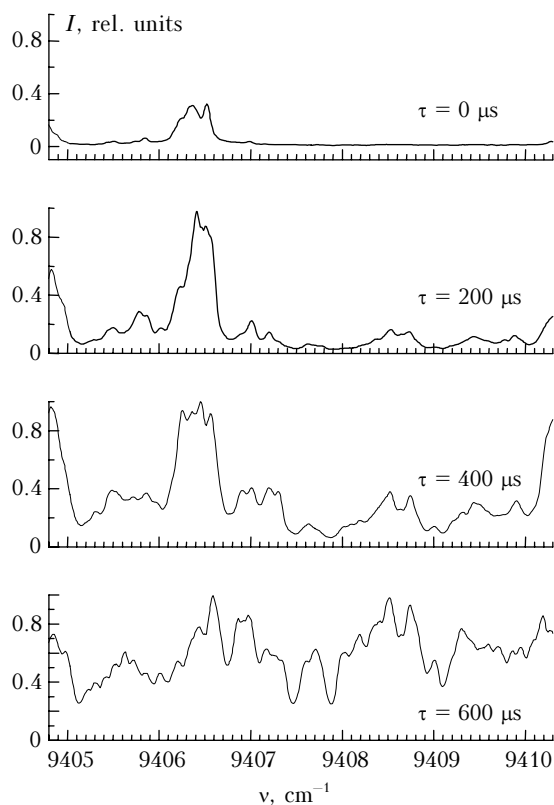


Fig. 4. IC spectrum of  $C_2$  radicals excited by laser spark in the  $9405\text{--}9410\text{ cm}^{-1}$  range.

As the result of the performed analysis, 88 absorption lines from those registered in the range  $9360\text{--}9460\text{ cm}^{-1}$  were referred to the  $C_2$  radical (see Table).

Table. Wavenumbers of  $C_2$  absorption line centers within the  $9385\text{--}9450\text{ cm}^{-1}$  range

Wavenumber, $\text{cm}^{-1}$	Wavenumber, $\text{cm}^{-1}$ (Ref. 15)	Electronic and vibrational bands	Rotational line
1	2	3	4
9387.848(8)	7.8221(114)	$b-a\ 5-2$	Q1(17)
9388.244(9)	8.2372(463)	$b-a\ 5-2$	R2(26)
9390.305(9)	0.3133(193)	$b-a\ 5-2$	R1(26)
9390.521(10)	0.5302(133)	$b-a\ 4-1$	Q3(39)
9391.292(7)	1.2678c	$b-a\ 4-1$	P3(32)
9391.736(8)*	1.7843c	$b-a\ 5-2$	P2(10)
9392.168(12)	2.1346c	$b-a\ 3-0$	Q2(53)
9392.311(11)*	2.2760c	$b-a\ 3-0$	Q1(53)
9392.429(10)*	2.4100(299)	$b-a\ 4-1$	P2(32)
9392.576(9)*	2.5663(107)	$b-a\ 4-1$	Q2(39)
9393.132(10)	3.1173(81)	$b-a\ 4-1$	Q1(39)
9393.501(10)	3.4898(64)	$b-a\ 5-2$	Q3(15)
9394.073(9)	4.0682(154)	$b-a\ 4-1$	P1(32)
9397.031(11)*	7.0160c	$b-a\ 5-2$	P1(10)
9397.278(10)	7.2735(107)	$b-a\ 5-2$	Q2(15)
9399.648(10)	9.6413(113)	$b-a\ 5-2$	R3(24)
9399.810(11)*	9.8082c	$b-a\ 5-2$	P3(8)
9400.181(11)	0.1695(107)	$b-a\ 5-2$	Q1(15)
9401.258(9)	1.2537(64)	$b-a\ 5-2$	R2(24)
9403.520(8)*	3.5086(114)	$b-a\ 5-2$	R1(24)
	3.5526c	$b-a\ 5-2$	Q3(13)
9404.076(10)	4.1010c	$b-a\ 5-2$	P2(8)
9405.090(9)	5.1019(82)	$A-X\ 2-1$	P(22)
9407.419(8)	7.4163(35)	$A-X\ 2-1$	Q(28)
9407.701(15)*	7.6623(150)	$b-a\ 5-2$	Q2(13)
9407.827(10)*	7.8303(18)	$A-X\ 1-0$	P(38)
9409.041(12)	9.0612(60)	$A-X\ 2-1$	R(36)
9409.544(10)*	9.5841c	$b-a\ 5-2$	P(36)
9410.462(8)	0.4412c	$b-a\ 5-2$	P1(8)
9411.032(10)*	1.0378(146)	$b-a\ 5-2$	R3(22)
9411.147(7)*	1.1464(90)	$b-a\ 5-2$	Q1(13)
9412.014(9)	2.0096(147)	$b-a\ 5-2$	Q3(11)
9412.416(10)	2.4204(438)	$b-a\ 4-1$	R3(46)
9412.816(8)	2.7814(225)	$b-a\ 5-2$	R2(22)
9413.061(9)	3.0725(223)	$b-a\ 4-1$	R2(46)
9414.165(8)	4.2021c	$b-a\ 4-1$	R1(46)
9414.820(15)	4.8510c	$b-a\ 5-2$	P2(6)
9415.256(11)*	5.2250(124)	$b-a\ 5-2$	R1(22)
9415.568(9)	5.5844c	$b-a\ 3-0$	R2(60)
9416.420(11)	6.3943c	$b-a\ 3-0$	R3(60)
9416.624(9)	6.6152(101)	$b-a\ 5-2$	Q2(11)
9418.400(9)	8.3906(119)	$b-a\ 4-1$	Q3(37)
9418.890(15)*	8.8560(13)	$A-X\ 1-0$	Q(44)
9419.689(10)	9.6662c	$b-a\ 4-1$	P3(30)
9419.824(12)	9.811c	$b-a\ 5-2$	Q3(9)
9420.520(8)	0.4902(157)	$b-a\ 4-1$	Q2(37)
9420.800(11)*	0.7906(57)	$b-a\ 5-2$	Q1(11)
9420.905(10)*	0.8985(127)	$b-a\ 4-1$	P2(30)
9421.168(10)	1.1433(98)	$b-a\ 4-1$	Q1(37)
9422.702(12)*	2.6868(126)	$b-a\ 4-1$	P1(30)
9422.787(10)*	2.7765c	$b-a\ 5-2$	P1(6)
9422.860(12)*	2.8446(252)	$b-a\ 5-2$	R2(20)
9423.054(10)	3.082c	$b-a\ 5-2$	Q3(7)
9423.843(9)	3.8082c	$b-a\ 5-2$	Q3(7)

Table continued

1	2	3	4
9424.030(8)	4.0183c	<i>b-a</i> 5-2	Q2(9)
9425.032(9)	5.0224c	<i>b-a</i> 3-0	P3(44)
9425.555(11)	5.5435(144)	<i>b-a</i> 5-2	R1(20)
9425.756(10)	5.7440c	<i>b-a</i> 3-0	P2(44)
9426.766(11)	6.7694c	<i>b-a</i> 5-2	Q3(5)
9426.926(12)	6.9233c	<i>b-a</i> 3-0	P1(44)
9428.464(9)*	8.4773c	<i>b-a</i> 3-0	Q3(51)
9429.282(8)	9.2816(141)	<i>b-a</i> 5-2	R3(18)
9429.836(7)	9.8575c	<i>b-a</i> 5-2	Q2(7)
9430.129(9)*	0.1204(67)	<i>A-X</i> 2-1	P(20)
9430.197(12)*	0.1890c	<i>b-a</i> 3-0	Q2(51)
9430.361(11)	0.3741c	<i>b-a</i> 3-0	Q1(51)
9432.412(10)*	1.4123(35)	<i>A-X</i> 2-1	Q(26)
9433.910(11)	3.8912(74)	<i>A-X</i> 2-1	R(34)
9434.088(13)	4.0746c	<i>b-a</i> 5-2	Q2(5)
9434.421(10)	4.4160(173)	<i>b-a</i> 5-2	R1(18)
9436.150(12)	6.1365(117)	<i>b-a</i> 5-2	R3(16)
9436.444(11)*	6.4199c	<i>b-a</i> 5-2	Q1(7)
9438.540(9)	8.5414(137)	<i>b-a</i> 5-2	R2(16)
9440.014(10)	0.0374(398)	<i>b-a</i> 4-1	R3(44)
9440.754(7)	0.7613(255)	<i>b-a</i> 4-1	R2(44)
9441.465(11)	1.4346c	<i>b-a</i> 5-2	R3(14)
9441.933(10)	1.9183(219)	<i>b-a</i> 4-1	R1(44)
9442.670(11)*	2.6626c	<i>b-a</i> 5-2	Q1(5)
9444.175(10)*	4.1587c	<i>b-a</i> 5-2	R2(14)
9444.823(10)	4.8040(75)	<i>b-a</i> 4-1	Q3(35)
9445.171(10)	5.1711c	<i>b-a</i> 5-2	R3(12)
9446.230(10)	6.2070c	<i>b-a</i> 5-2	R3(6)
9446.618(10)	6.6341(120)	<i>b-a</i> 4-1	P3(28)
9446.987(10)	6.9758(96)	<i>b-a</i> 4-1	Q2(35)
9447.281(7)	7.2829c	<i>b-a</i> 5-2	R3(10)
9447.720(10)	7.6958(101)	<i>b-a</i> 4-1	Q1(35)
9447.972(6)	7.9676(120)	<i>b-a</i> 4-1	P2(28)
	7.9846c	<i>b-a</i> 5-2	R1(14)
9448.350(7)	8.2830c	<i>b-a</i> 5-2	R2(12)
9449.927(15)	9.8842(116)	<i>b-a</i> 4-1	P1(28)

Note. Wavenumbers of line centers marked by "\*" were determined from doublet lines; wavenumbers marked by "c" were calculated in this work.

Most spectral lines were observed for transitions between electronic states  $b^3\Sigma_g^-$  and  $a^3\Pi_u$ ; rotational lines of 3-0, 4-1, and 5-2 transitions were identified. The majority of lines for the last vibrational band were determined for the first time. Besides transitions from the first excited electronic state, absorption lines for the transition from the ground state  $X^1\Sigma_g^+$  to the excited one  $A^1\Pi_u$  appeared in the spectrum.

The performed investigations have shown a high efficiency of the intracavity laser spectroscopy technique in studying absorption spectra of laser-spark excited molecules.

### Acknowledgments

The authors are grateful to Corresponding Member of RAS S.D. Tvorogov for his support and attention to the work.

This work was supported by Russian Foundation for Basic Research (Grant No. 05-03-32782) and the Program 2.10 "Optical spectroscopy and frequency standards."

### References

1. F. Brech and L. Cross, *Appl. Spectrosc.* **16**, No. 1, 59-66 (1962).
2. D.W. Hahn, A.W. Miziolek, and V. Palleschi, *Appl. Opt.* **42**, No. 30, 5937-5938 (2003).
3. D.A. Rusak, B.C. Castle, B.W. Smith, and J.D. Winerfordner, *Crit. Rev. Anal. Chem.* **27**, No. 4, 257-290 (1997).
4. K. Song, Y.-I. Lee, and J. Sneddon, *Appl. Spectrosc. Rev.* **32**, No. 3, 183-235 (1997).
5. J. Sneddon and Y.-I. Lee, *Anal. Lett.* **32**, No. 11, 2143-2162 (1999).
6. V.S. Burakov, P.A. Naumenkov, and S.N. Raikov, *Opt. Commun.* **80**, No. 1, 26-30 (1990).
7. V.S. Burakov, S.N. Raikov, and N.V. Tarasenko, *Zh. Prikl. Spektrosk.* **64**, No. 3, 281-290 (1997).
8. L.A. Pakhomycheva, E.A. Sviridenkov, A.F. Suchkov, and L.V. Titova, *Pis'ma Zh. Eksp. Teor. Fiz.* **12**, Is. 2, 60-63 (1970).
9. V.V. Osipov, V.I. Solomonov, V.V. Platonov, O.A. Snigireva, M.G. Ivanov, and V.V. Lisenkov, *Quant. Electron.* **35**, No. 5, 467-473 (2005).
10. T.M. Petrova and L.N. Sinitsa, *Atmos. Oceanic Opt.* **16**, No. 11, 937-940 (2003).
11. T.M. Petrova, Yu.A. Poplavskii, and L.N. Sinitsa, *Opt. Spektrosk.* **98**, No. 3, 396-401 (2005).
12. Yu.Ya. Kuzyakov and E.N. Moskvitina, *Vestn. Mosk. Univ, Ser. 2* **42**, No. 3, 162-166 (2001).
13. A.V. Orden and R.J. Saykally, *Chem. Rev.* **98**, No. 6, 2313 (1998).
14. K.-P. Hubert and G. Herzberg, *Constants of Diatomic Molecules* [Russian translation] (Mir, Moscow, 1984), 203 pp.
15. C. Amiot, J. Chauville, and J.-P. Maillard, *J. Mol. Spectrosc.* **75**, No. 1, 19-40 (1979).
16. J. Chauville and J.-P. Maillard, *J. Mol. Spectrosc.* **68**, No. 2, 399-411 (1977).
17. S.P. Davis, M.C. Abrams, J.G. Phillips, and M.L.P. Rao, *J. Opt. Soc. Am. B* **5**, No. 10, 2280-2285 (1988).
18. M. Douay, R. Nietmann, and P.F. Bernath, *J. Mol. Spectrosc.* **131**, No. 2, 250-260 (1988).